An official publication of the International Society for Energy, Environment and Sustainability (ISEES)

Journal of Energy and Environmental Sustainability

Journal homepage : www.jees.in

Numerical Investigation of Swirling Hydrogen Flames: Effect of Swirl and Fuel Jet in Coherent Structures

V. Suresh Balaji [1], Ashoke De [*1], Santanu De[2]

[1]Department of Aerospace Engineering, [2]Department of Mechanical Engineering Indian Institute of Technology, Kanpur-208 016, India

ARTICLE INFO

Received : 03 September 2015
Revised : 09 October 2015
Accepted : 10 October 2015

Keywords:
Swirling hydrogen flames,
Large Eddy Simulation,
Precessing Vortex Core

ABSTRACT

The present work reports on the numerical investigation of turbulent swirling flames using Large Eddy Simulation (LES) methodology in conjunction with presumed shape PDF (Probability Density Function) based combustion models. The LES with dynamic-smagorinsky eddy viscosity model is used to study the different complex unsteady structures involved in the flow field. Sydney swirl burner, which is considered as a reliable benchmark for numerical studies in swirling flames, is chosen as a test case. Two isothermal and three reacting test cases are considered for the present study. In the isothermal calculations, a precession vortex core is accurately captured. The precession vortex core structures, responsible for the instability in hydrogen-methane reacting cases, are analyzed using different visualization techniques. Phase averaging technique is also used to analyze the different repeated coherent structures responsible for the instability in the flow field.

© 2016 ISEES, All rights reserved

1. Introduction

Efficient use of energy and reduction of emissions are the most essential design parameters for any engineering appliances, especially in propulsive devices. This gives rise to the need for constant progress in the research areas of combustion to meet the stringent emission regulations and environment requirements. From the past, fossil fuel has been the attracting fuel for combustion devices. However, the emissions of unburned hydro carbons, nitrogen oxides, carbon monoxide and other pollutants create the need for an alternate for fossil fuel application. Use of hydrogen fuel instead of fossil fuels is one of the efficient ways of handling the present day crises in the energy and to reduce the impact of emissions on environment. However, the use of pure hydrogen as a fuel for combustion systems is highly inclined towards safety issues owing to highly inflammable nature of hydrogen, particularly during transportation processes. So, by blending hydrogen with other fossil fuels, this inflammable risk factor can be reduced. Besides, combustion in swirling flows is one of the most widely used techniques as it shows a significant enhancement in stability of the flame with the help of recirculation zones. Besides enhancing the stability, better mixing is achieved which gives rise to the increase in combustion efficiency thereby reducing the pollutant emissions. In addition to that, the flame length is reduced by enhancing mixing, which results in reduction in combustion chamber length. However, swirling flow coherent structures such as Precessing vortex core (PVC). Even though it helps in large scale turbulent mixing, PVC also produces undesirable noises and instability of the flame. So, it is very much essential to have deeper insight to the analysis of the swirling flows in order to have an optimized design and improved combustion efficiency. So, to have a sustainable combustion technology, combustion of hydrogen blended fuels in swirling flows is one of the attractive methods in the research areas of hydrogen energy.

Several studies are reported in the literature on non premixed combustion of hydrogen blended fuels. Dinesh et al. (2012) studied the combustion of syngas with different proportions of hydrogen blended with NO and CO. And it was reported that there was a significant change in unsteady and steady flame temperature with the different proportion of hydrogen in the fuel. In the contest of swirling flames with hydrogen, LES in combination with presumed shape PDF approach was applied to Hydrogen-methane swirling flame by Malasekara et al. (2010). It was concluded in that work that LES could be a very useful tool in accurate modeling of combustion characteristics and its capability was expected to grow in future. In another study, Dinesh et al. (2006) has studied a single hydrogen-methane flame from Sydney swirl burner using LES technique and observed some discrepancy in the mixture fraction predictions. In a follow up work, Dinesh et al. (2009) studied the instability mechanism associated with three methane-hydrogen flames of Sydney swirl burner. Kempf et al. (2008) studied one pure methane case and two methane-hydrogen case from Sydney swirl burner with two different LES programs with different SGS models and numerical techniques to have a code-independent analysis of these flames. Stein and Kempf (2007) studied one pure methane case and one methane-hydrogen case, and revealed some challenging features and difficulties of LES in predicting the complex flow structures.

* *Corresponding Author: E-mail address: ashoke@iitk.ac.in, Tel.: +91-512-2597863*

© 2016 ISEES All rights reserved

Besides, some non-hydrogen reacting cases are studied using LES and reported in the literature. El-Asrag and Menon (2005) reported a study on reactive swirling flame database of Sydney Swirl burner using LES with sub grid mixing and combustion model based on the Linear Eddy Mixing approach. The recirculation zone size, flame structure and its length were studied. Dinesh et al. (2005) studied two swirling flames and the different dynamics involved in the flow are explored. Hu et al. (2008) studied swirling non premixed flame using LES technique for validation of different sub-grid scale models. LES technique in combination with PDF based approach is applied by James et al. (2007) to have comparative study on the pure methane and methane-air flames. The model predicted the flow physics well and the different coherent structures were captured. Overall, it was concluded that LES is a very useful tool in accurate modeling of non premixed flames and expected to grow in future as it could produce an accurate amount of flow characteristics.

In addition, several studies are reported in literature on the swirling reacting and non-reacting flows. Syred and Beer (1974) presented a detailed review on combustion in swirling flows. Lilly (1977) reported a review on swirl flows in combustion and summarized the advancements in experimental techniques and numerical predictions in dealing with swirling flows. Candel et al. (2014) presented a complete review on the dynamics of the swirling flow and the different issues to be studied further. Malasekara et al. (2008) reported a study on swirling non premixed isothermal jets using LES. Experimentally observed vortex break down and different structures were successfully reproduced in the LES simulations and the potential for LES in industrial applications was emphasized. Dinesh et al. (2009) studied an isothermal flame from Sydney swirl burner database and proved that LES is adequately accurate and computationally efficient than Direct Numerical Simulation. Another study is reported in isothermal jet of Sydney swirl burner by Yang et al. (2010). Proper Orthogonal decomposition is applied to study the different coherent structures involved in the flow. Another work by Ranga Dinesh et al. (2005) reports for the need of further improvement in the LES technique to capture the different dynamics of the flow. The recirculation zone, vortex break down and precessing vortex core are studied by Yang and Soren (2012). Comparative study between Reynolds Average Navier Stokes formulation and LES technique is reported for one isothermal flow by Yang and Soren (2012). In this study, it was observed that the vorticity fields captured were different for LES and RANS technique with LES captured the most realistic predictions. More recently, De and Acharya (2012) investigated both non-reacting and reacting methane-hydrogen premixed flames using LES, which also exhibit the capability of LES technique in predicting such flows. Moreover, several experimental studies are reported in the literature in the context of swirling flames (Al-abdeli and Masri, 2003, 2004; Masri et al., 2004; Al-abdeli et al., 2006).

From the above review, it can be concluded that LES has been proved to be a powerful technique in dealing with turbulent swirling flames. Also, from the literature, it is seen that the database of Sydney swirl burner offers challenging flames with various complexity and interesting flow behaviors. Most of the studies in the context of swirling flows are inclined towards non reacting flows and reacting flows of non-hydrogen flames. Very few studies are reported in the context of swirling hydrogen blended flames, while only few studies reported on the instability analysis of these flames. However, none of the studies is reported on the effects of interaction of swirl and the fuel jet velocity in the instability of hydrogen blended swirling flames. In this study, the effect of swirl number and the fuel jet velocity in the instability of hydrogen based swirling flames is analyzed using LES technique with presumed shape PDF approach. To do so, two non-reacting cases and three hydrogen cases from Sydney swirl database are simulated and analyzed. Firstly, the simulation of non-reacting cases provides the basic idea on the hydrodynamic behavior of the flow field followed by the simulations of methane-hydrogen case which presents the vital information on the effect of hydrogen addition. Finally, the simulation of three hydrogen cases, in which the first two cases contains same fuel jet velocity with different swirl number and the last two cases contains same swirl number with different fuel jet velocities, are carried out. This study provides the effect of swirl number and the fuel jet velocity in the turbulent structures of hydrogen based swirling flames. Phase averaging technique is used to visualize the repeated structures, in order to explore the interactions between fuel and swirling jet.

2. Numerical Details

2.1. Flow modeling using LES

In order to model the turbulence, LES is used where the large scale structures are resolved and the small scale structures are modeled. Hence, the filtered governing equations for the conservation of mass, momentum, energy and species transport are solved in the present work (Bhaya et al., 2014). Dynamic Smagorinsky model is used for sub-grid stress modeling (Smagorinsky, 1963; Germano et al., 1991), where the gradient approximation is invoked to relate the unresolved stresses to resolved velocity field and given as:

$$\widetilde{u_i u_j} - \tilde{u}_i \tilde{u}_j = -2\nu_t \bar{S}_{ij} \tag{1}$$

$$\text{Where } \nu_t = C_s^2 (\Delta)^2 \left|\bar{S}\right| \tag{2}$$

$$\bar{S}_{ij} = \left(\frac{\partial \bar{u}_i}{\partial x_j} + \frac{\partial \bar{u}_j}{\partial x_i} \right) \tag{3}$$

$$\left|\bar{S}\right| = \sqrt{2\bar{S}_{ik}\bar{S}_{ik}} \tag{4}$$

and S is the mean rate of strain. The coefficient C_s is evaluated dynamically (Smagorinsky, 1963; Germano et al., 1991).

2.2 Combustion modelling: Steady Flamelet (SF) Model

In this CFD solution, the chemistry is completely described by the two quantities (i.e.) the mixture fraction f and the scalar dissipation rate χ. The scalar dissipation term is an equivalent term for strain rate and represents the departure from equilibrium. This reduction of two variables enables flamelet calculations to be pre-calculated and stored in table which reduces the computational cost. Hence, by transferring the equation from physical space to mixture fraction space, a simplified set of equations in mixture fraction space are solved. Therefore, N equations are solved for species mass fraction along with one equation for temperature as given below:

$$\frac{1}{2}\rho\chi\frac{\partial^2 Y_i}{\partial f^2} + S_i = 0 \tag{5}$$

$$\frac{1}{2}\rho\chi\frac{\partial^2 T}{\partial f^2} - \frac{1}{C_p}\sum_i H_i S_i + \frac{1}{2C_p}\rho\chi\left[\frac{\partial C_p}{\partial f} + \sum_i C_{p,i}\frac{\partial Y_i}{\partial f}\right]\frac{\partial T}{\partial f} = 0 \tag{6}$$

where Y_i, T, ρ, S, are the species mass fraction, temperature, density and chemical production rate of species respectively. Also, C_p and $C_{p,i}$ are the mixture–averaged specific heat and species specific heat respectively.

The scalar dissipation rate is defined as, $\chi = 2D\left|\nabla f\right|^2$ (7)

where D is the diffusion co efficient. The scalar dissipation rate at the flame surface χ_{st} is closed by

$$\chi_{st} = \frac{a_s \exp\left(-2\left[erfc^{-1}\left(2f_{st}\right)\right]^2\right)}{\pi}$$

where X_{st} is the scalar dissipation rate at $f = f_{st}$

a_s is the characteristic strain rate

f_{st} is the stoichiometric mixture fraction

$erfc^{-1}$ is the inverse complementary error function.

3. Test Case

The schematic view of the Sydney swirl burner is shown in Fig. 1(a). The central fuel jet has a diameter of 3.6 mm. The central jet is surrounded with a ceramic bluff-body of 50 mm in diameter. The swirling air flow is made to come out through the annulus of diameter 5 mm. The swirling flow consists of two components: the annular axial velocity Us and the annular swirling velocity Ws. The whole setup is placed into a wind tunnel with 130 X 130 mm square cross section sides which delivers an external co flow ambient velocity Ue, which is kept constant (Masri et al., 2004). Three tangential acclivitous ports with a diameter 7 mm each are used to create the swirl component. The swirl strength is quantified by the geometrical swirl number S_g (S_g=W_s/U_s). The characteristics of the swirling flow are altered by changing these three bulk velocities and also the geometrical swirl number. The test case and the corresponding boundary conditions used are tabulated in the Table 1.

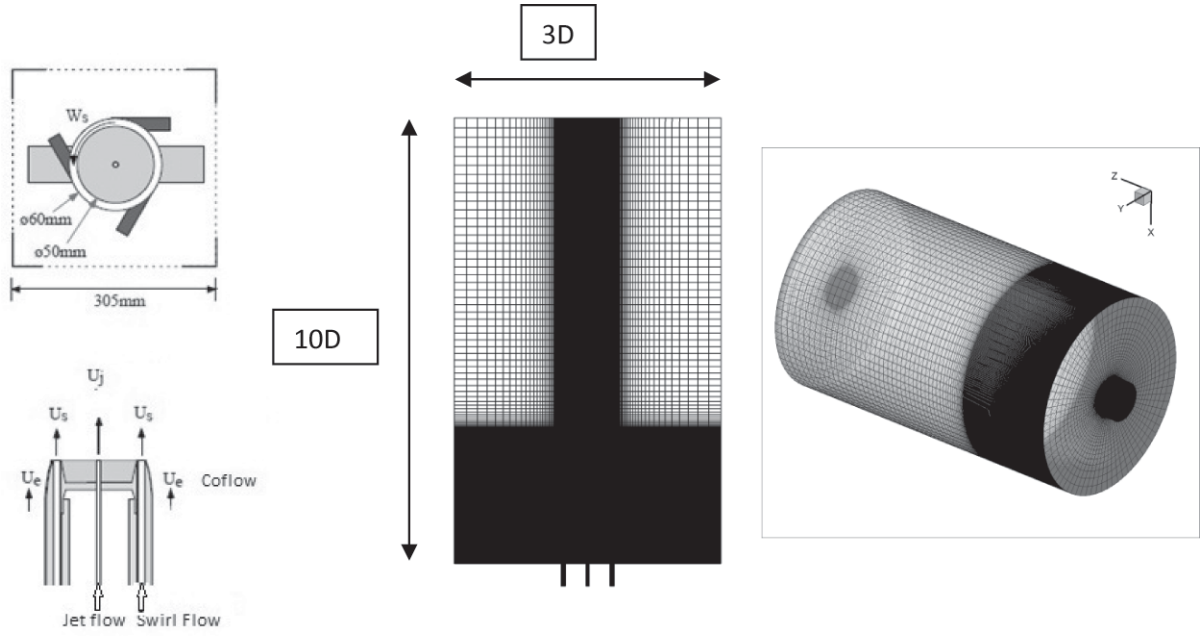

Figure 1(a): Schematic of Sydney swirl burner and LES grid

k_{tur}

Table 1: Boundary Conditions for the simulated cases

	CASE	FUEL	U_j	U_s	W_s	U_e	S_g
Isothermal case	N29S054	-	66	29.7	16	20	0.54
	N16S159	-	66	16.26	25.85	20	1.59
Methane-Hydrogen case	SMH1	CH4 - H2 (1:1)	140.8	42.8	13.8	20	0.3
	SMH2		140.8	29.7	16	20	0.5
	SMH3		226	29.7	16	20	0.5

4 Computational Domain

Sydney swirl burner is used as a test case for studying the combustion in swirling flows. The three dimensional grid comprises of 2.8M cells and is extended upto 500 mm in the downstream direction, 150 mm in radial direction and 25 mm in the upstream direction. A non uniform node distribution is used with 335 nodes in the axial direction, 114 nodes in the radial direction and 80 nodes in the azimuthal direction. The 'O' grid is used near the central jet to have a uniform distribution of grid in the azimuthal direction as depicted in Fig. 1(a). This grid is used for the simulation of cold flow and pure methane case. For the hydrogen-methane case, the grid comprises of 5.9M cells with 682 nodes in the axial direction, 114 nodes in the radial direction and 80 nodes in the azimuthal direction.

The simulations are carried out using the commercial software package ANSYS FLUENT-15.0 (Ansys, 2010). The convective term in the momentum equation is discretized using second order bounded central differencing scheme while the second order discretization is consistently used for all the terms and a pressure based segmented algorithm is used for solving all the equations. The turbulence chemistry interaction is modeled using steady Flamelet model and GRI3.0 mechanism (Smith et al., 1999), with 53 species and 325 reactions, is used to represent the chemistry. The PISO algorithm is used in pressure velocity coupling. The boundary condition at the outlet is set to pressure outlet while the symmetry boundary condition is used at the radial boundary. The boundary condition at the fuel inlet and swirl inlet is generated using 1/7- power law profile.

5 Results & Discussion

5.1 Grid Resolution

The resolution of grid plays a predominant role in LES calculations in capturing the different flow structures involved in the flow. A lot of indicators are reported in the literature for determining LES grid resolution. In this study, two methods proposed by Pope (2000) and Celik at al. (2005) are used to find the quality of grid. In the first method as proposed by Pope (2000), to have good LES predictions, at-least 80% of the kinetic energy should be resolved. This is done by finding the ratio of turbulent kinetic energy, and the total turbulent kinetic energy, $k_{tot} = k_{tur} + k_{sgs}$ and the value is checked for the resolution of the grid. The k_{tur} is calculated from the predicted rms velocities and the k_{sgs} is calculated separately using a UDF during the iteration process (Bhaya et al., 2014). In addition to a LES test filter, the UDF uses the grid filter size and the test filter kinetic energy from the solver to calculate k_{sgs} using the formula (Bhaya et al., 2014)

$$k_{sgs} = \frac{\Delta_{sgs}}{\Delta_{test}} k_{test} \tag{9}$$

Figure 1(b) shows the grid resolution using this technique and it is confirmed that more than 85% of the turbulent kinetic energy is resolved throughout the domain especially in the shear layer region. Another method as proposed by Celik et al. (2005) uses eddy viscosity ratio as an

indicator for examining the grid resolution. The formulation of this method is given by

$$LES\_IQ = \frac{1}{1+0.05\left(\frac{\upsilon_{t,eff}}{\upsilon}\right)^{0.53}} \quad (10)$$

In this formulation $\upsilon_{t,eff}$ denotes the effective viscosity, which is the sum of laminar and turbulent viscosity, and υ denotes the laminar viscosity. The LES quality index should be greater than 0.8 for good LES predictions [33]. Fig. 1(b) shows the LES quality index distribution throughout the domain and it confirms the quality of the present grid.

5.2 Non-Reacting flow results

This section presents the computed results of two non reacting cases. Before presenting the analysis of hydrodynamic behavior of the flame, the present LES calculation is validated with the experimental measurements. Fig. 2(a) depicts the comparison of LES predictions with the experimental measurements of low swirl and high swirl cases at different axial locations. The predictions show overall good agreement with the experimental measurements both in upstream and downstream regions. The center line axial velocity near the burner is well capture in both low swirl and high swirl cases. At Z/D = 1.4, the central line negative velocity is captured well, which indicates that the recirculation zone is captured accurately. While looking at a single three dimensional stream trace from the fuel jet for these cases, it is observed that two distinct recirculation regions: one near the bluff body region and another

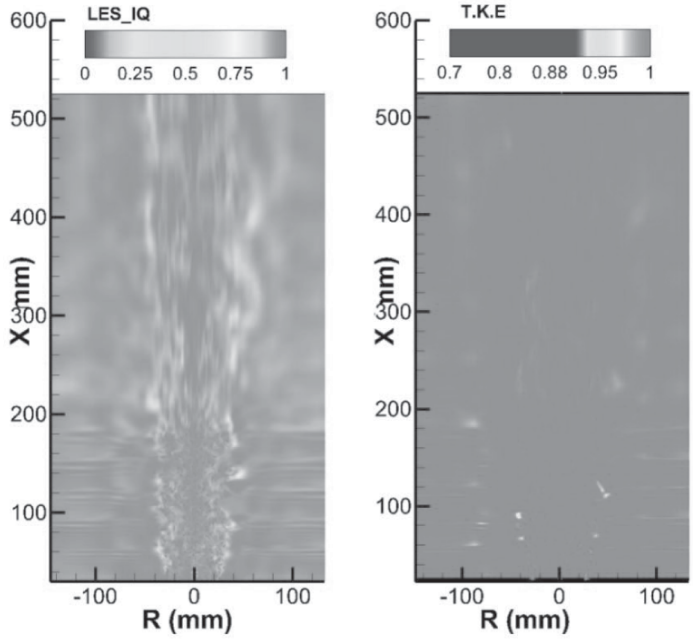

Figure 1(b): Resolution of Grid using LES quality criteria (Celik et al., 2005) (Left) and Resolution of the turbulent kinetic energy (Right) in the domain

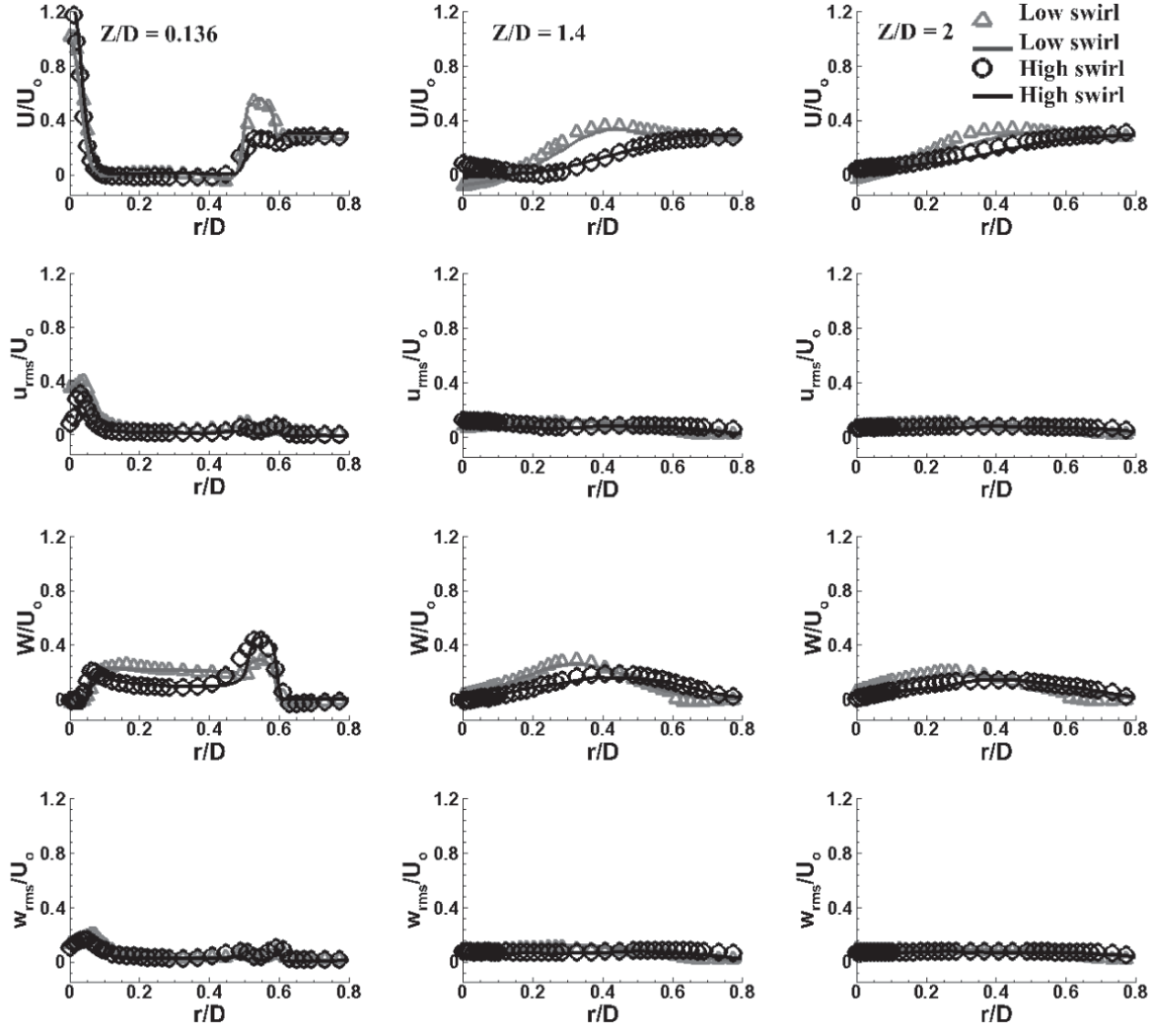

Figure 2(a): Radial plot of mean and rms velocity of non reacting case: Symbols are measurements and lines are predictions

one in the downstream position; whereas in the high swirl case, a single long recirculation region is captured. In the high swirl case, the axial momentum flux is lesser compared to the low swirl case. In addition, the tangential momentum flux is predominant in the high swirl case. This predominant tangential momentum and the adverse pressure gradient causes high swirl case with a single recirculation region.

Further, the detailed precessing vortex core (PVC) structure is visualized using the second eigen value method. Fig. 2(b) shows the comparison of PVC structures of both high and low swirl cases. The PVC structure is clearly visible in low swirl case whereas it diffuses much quickly in high swirl case. Further, Fast Fourier Transform (FFT) technique is used to analyze the frequency corresponding to the oscillation of this PVC structure. A clear peak of frequency at around 488Hz for high swirl case and two different peaks for low swirl case; one near bluff body region at around 162 Hz and another peak at around 325 Hz in the downstream position (Figs. 3(a-c)) are observed. This agrees with the two distinct structures in the low swirl case and a single long recirculation region of high swirl case.

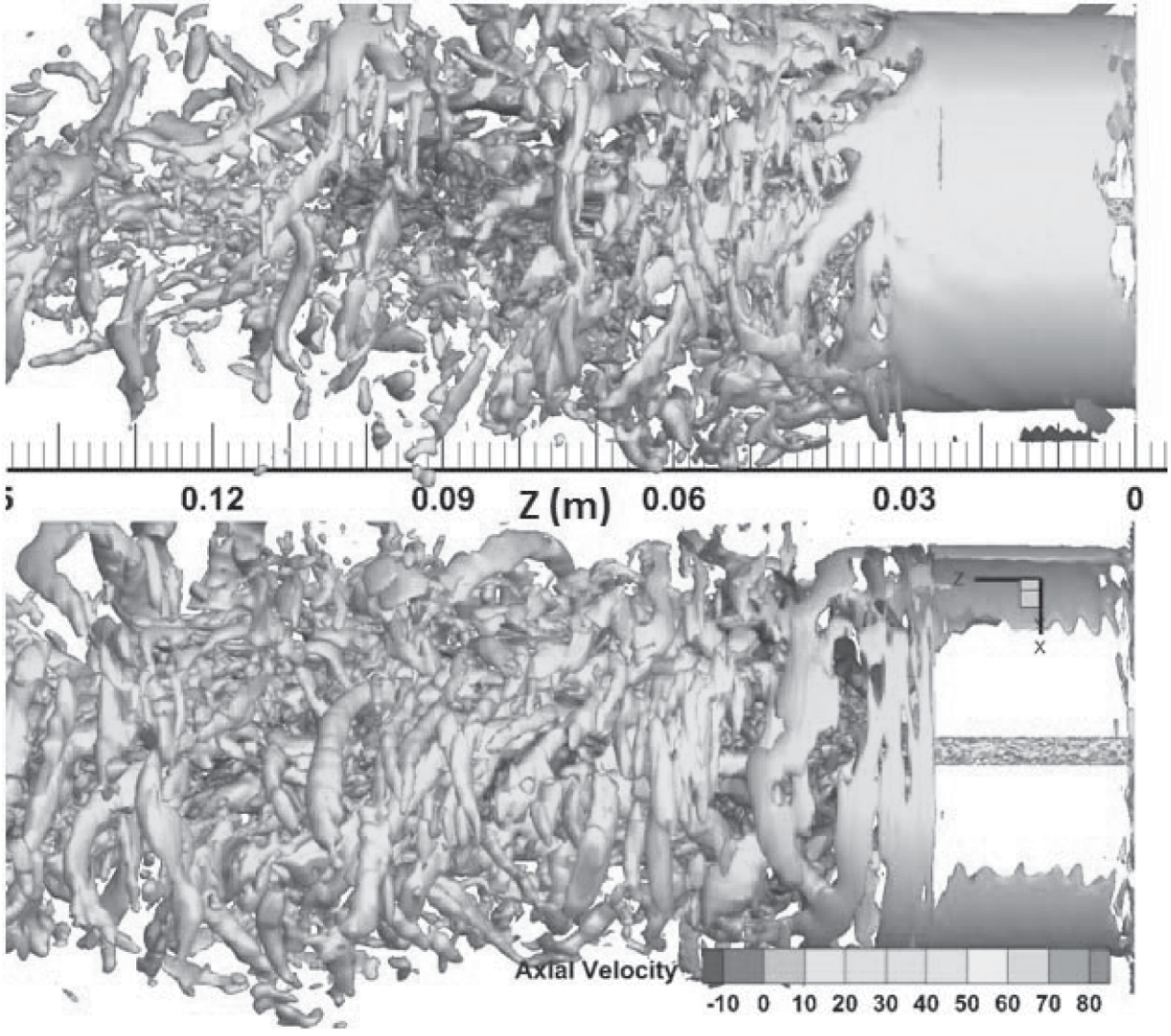

Figure 2(b): PVC structure visualization of non reacting case: Low swirl case (top), high swirl case (bottom)

Further, the inner structures responsible for this observed frequency are explored using phase averaging technique. Figs. 3(a-c) show the five phases of a complete cycle corresponding to two peaks of low swirl case and one peak of high swirl case respectively. And the each phase is averaged over four complete cycles to eliminate the high frequency oscillations. In Fig. 3(a) at phase 1, it clearly shows a formation of a vortex due to swirling air, induced behind the bluff body in both the sides of fuel jet. This shedding vortex, which grows in size by interacting with the smaller vortex formed, changes its shape in phase 2 due to the change in pressure fluctuations shown in Fig. 3(a). Fig. 3(b) shows the phase averaging data for second peak of low swirl case. The data presented here at each phase is averaged over five complete cycles to remove the high frequency oscillations. At phase 1, it clearly shows a formation of a vortex due to swirling air, induced behind the bluff body in both the sides in upstream position. This shedding vortex changes its shape in phase 2 due to the change in pressure fluctuations shown in Fig. 3(b). Then in phase 3, the same vortex grows in size and regains its shape in phases 4 and 5. The same characteristics are shown in both the sides. In addition to that, along the center line at a axial location of around Z/D= 1.5 from the exit plane, where the vortex breakdown phenomenon is observed, a clear change in the shape of recirculation bubble through different phases is observed. From the phase analysis, three distinct regions of repeating dominant structures is observed; the upstream position near the bluff body, downstream position along the center line and the neck region. The same pattern of interaction in the phase averaged data is observed for the second peak of low swirl. However, the interaction is more concentrated in the downstream position, where the distinct peak frequency is observed.

Fig. 3(c) shows the phase averaged instantaneous velocity vector of high swirl case representing the five phases of frequency. The dominant frequency is found at 488 Hz. Based on this frequency, each phase is averaged over five complete cycles and the result is presented here. In the figure, an already formed recirculation zone near the fuel jet along the axial line changes its shape through the different phases and regain its structure in the fifth phase. Similarly, a shedding vortex near the bluff body is getting elongated through third phase and regains its shape in the fifth phase. The PVC structure shown in Fig. 2(b) is compared with the

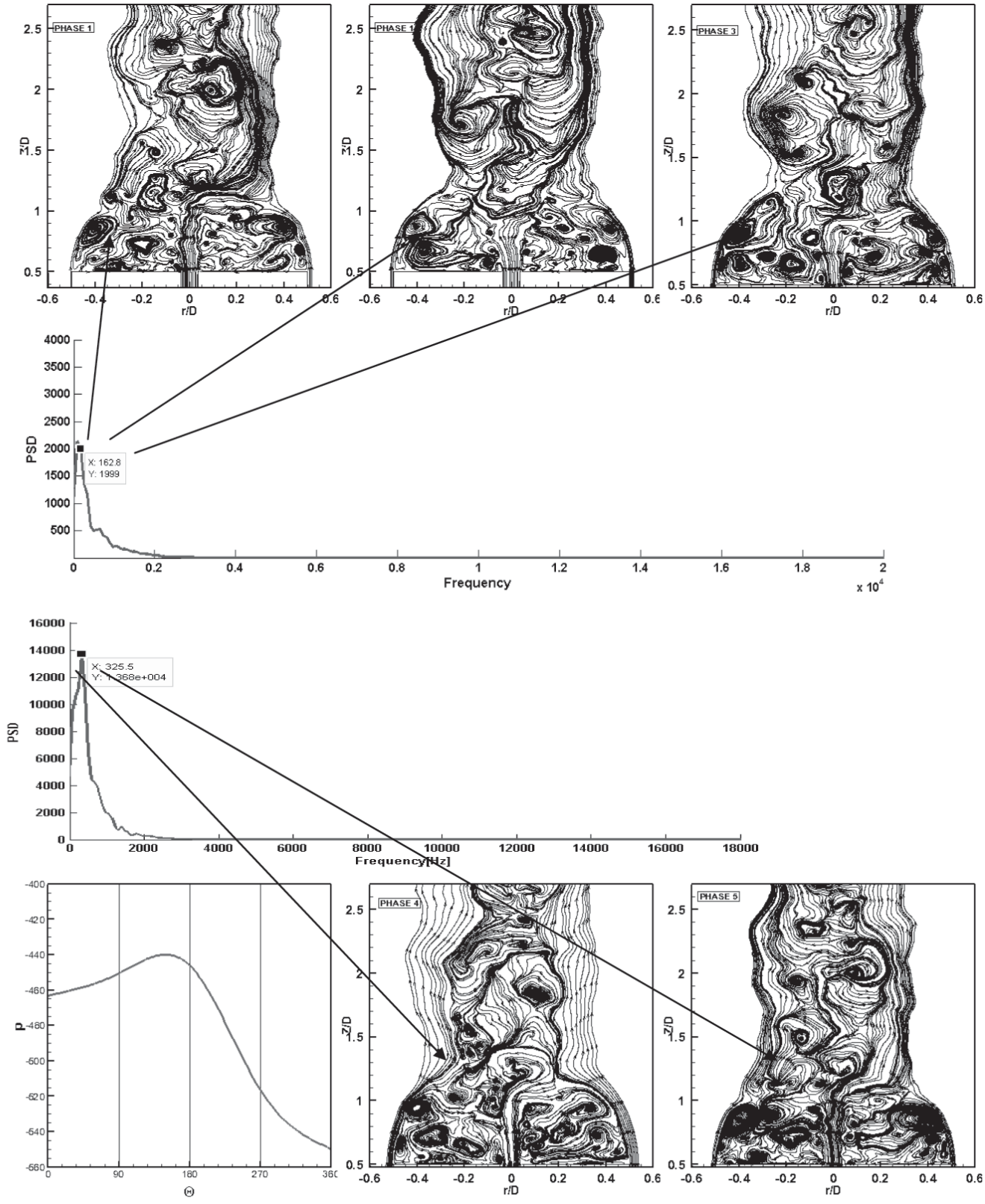

Figure 3(a): Phase averaged data for instantaneous flow from Phase 1-5 at an oscillation of 162Hz for Low swirl case

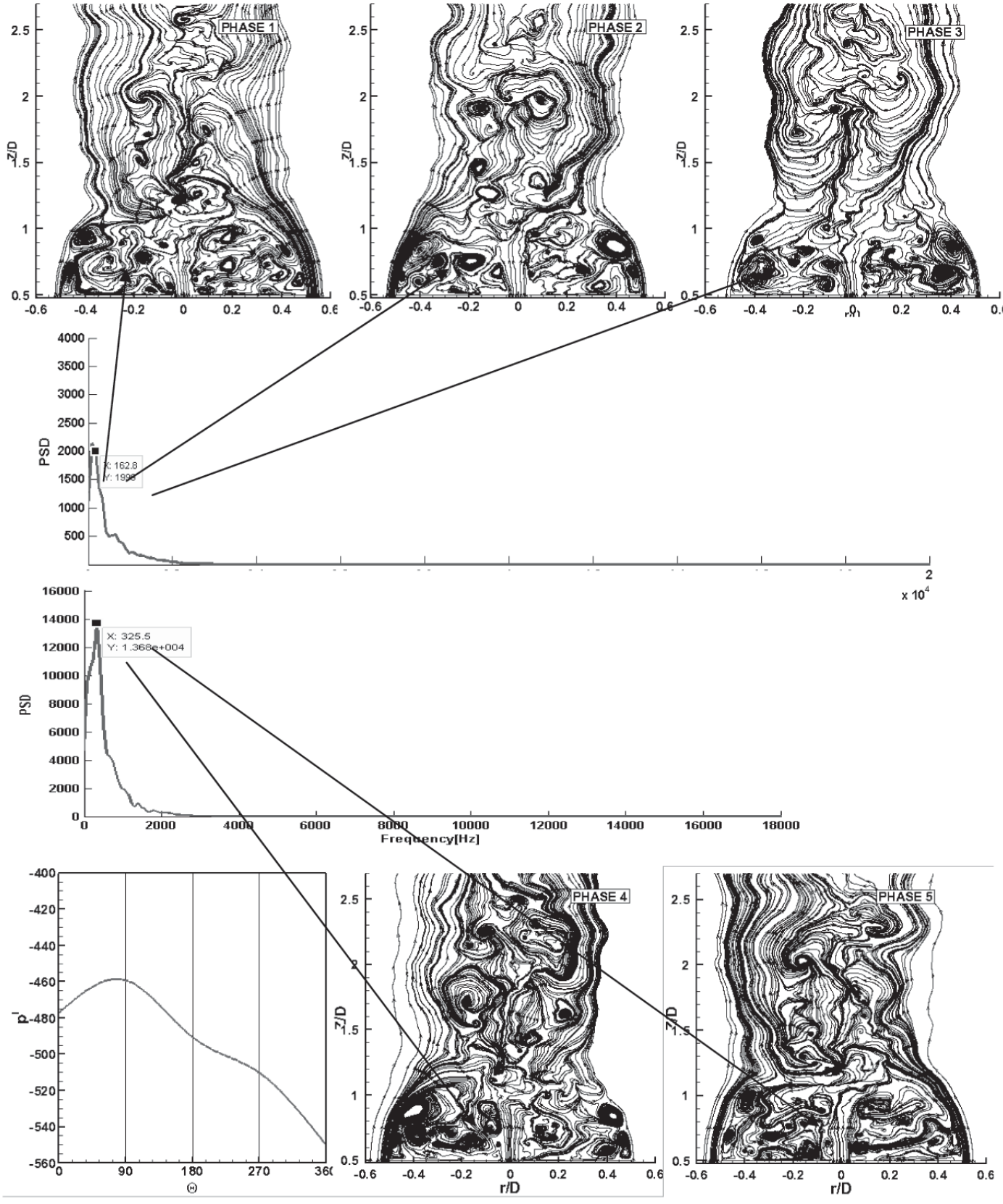

Figure 3(b): Phase averaged data for instantaneous flow from Phase 1-5 at an oscillation of 325Hz for Low swirl case

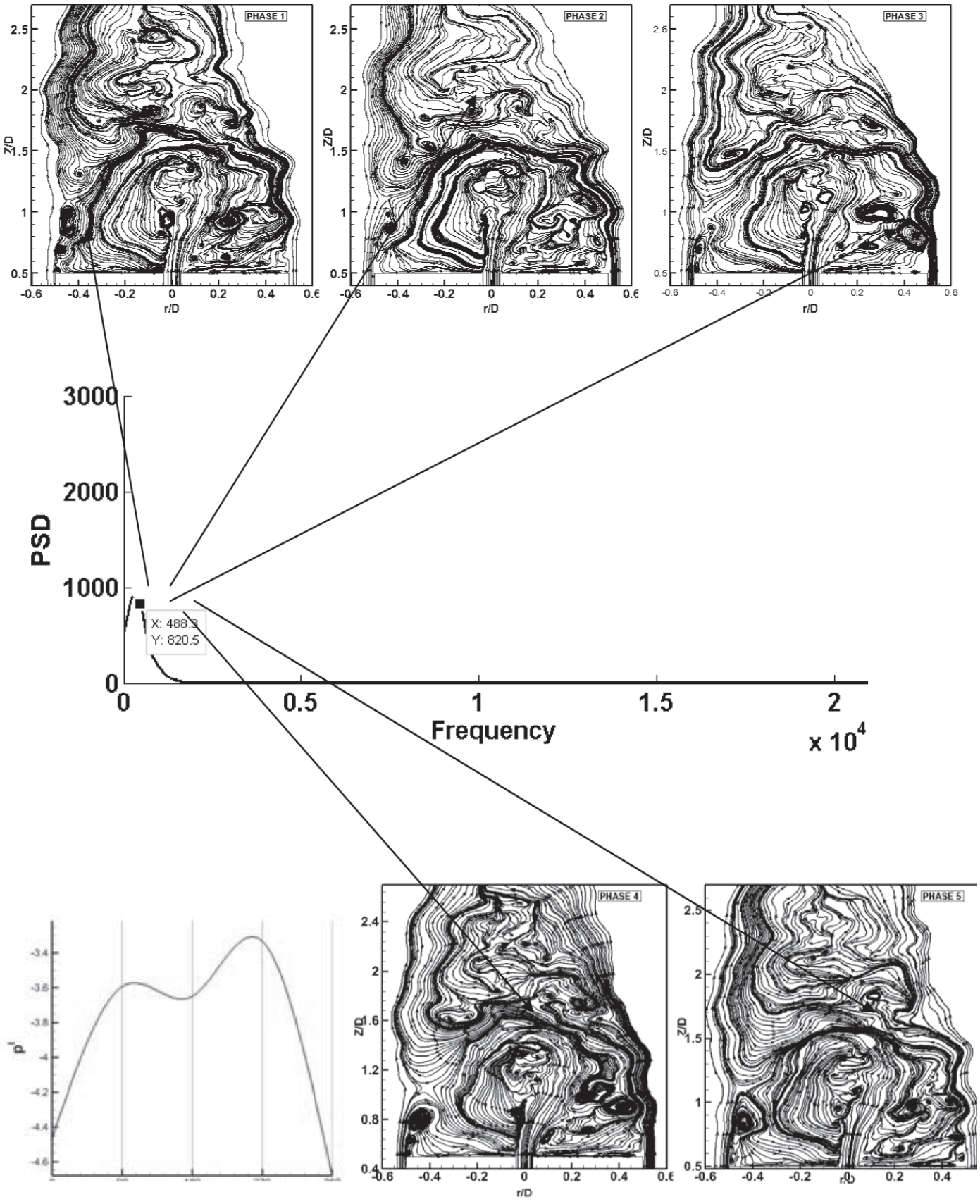

Figure 3(c): Phase averaged data for instantaneous flow from Phase 1-5 at an oscillation of 488Hz for High swirl case

phase averaged data. In low swirl case, due to the presence of secondary vortex breakdown bubble, the PVC structure is prolonged whereas in high swirl case the PVC structure diffuses quickly due to the absence of secondary recirculation region.

5.3 Reacting flow results

This section presents the flow characteristics of hydrogen blended flames.

5.3.1 Validation with Experimental Measurements

Initially, the pure methane flame is simulated followed by the hydrogen blended flames. Fig. 4(a) exhibits the mean and rms velocity predictions of the SMH1 case and SMH2 case respectively. The central line axial velocity at the burner exit is well predicted. At around Z/D = 0.4, the negative velocity is also predicted well. However, the recirculation bubble is extended upto Z/D = 0.8 and the negative velocity at this position is not captured. In the downstream position, the centre line velocity is over predicted and the prediction shows improvement in the radial positions. The predictions shows overall good agreement with the experimental measurements. The mean tangential velocity predictions shows overall good agreement with slight over prediction in the radial direction at about r/D = 0.2. The rms tangential velocity predictions also show good agreement with the experimental measurements. Some discrepancies are observed near the bluff body induced recirculation zone. But overall the predictions show good agreement with the experimental measurements.

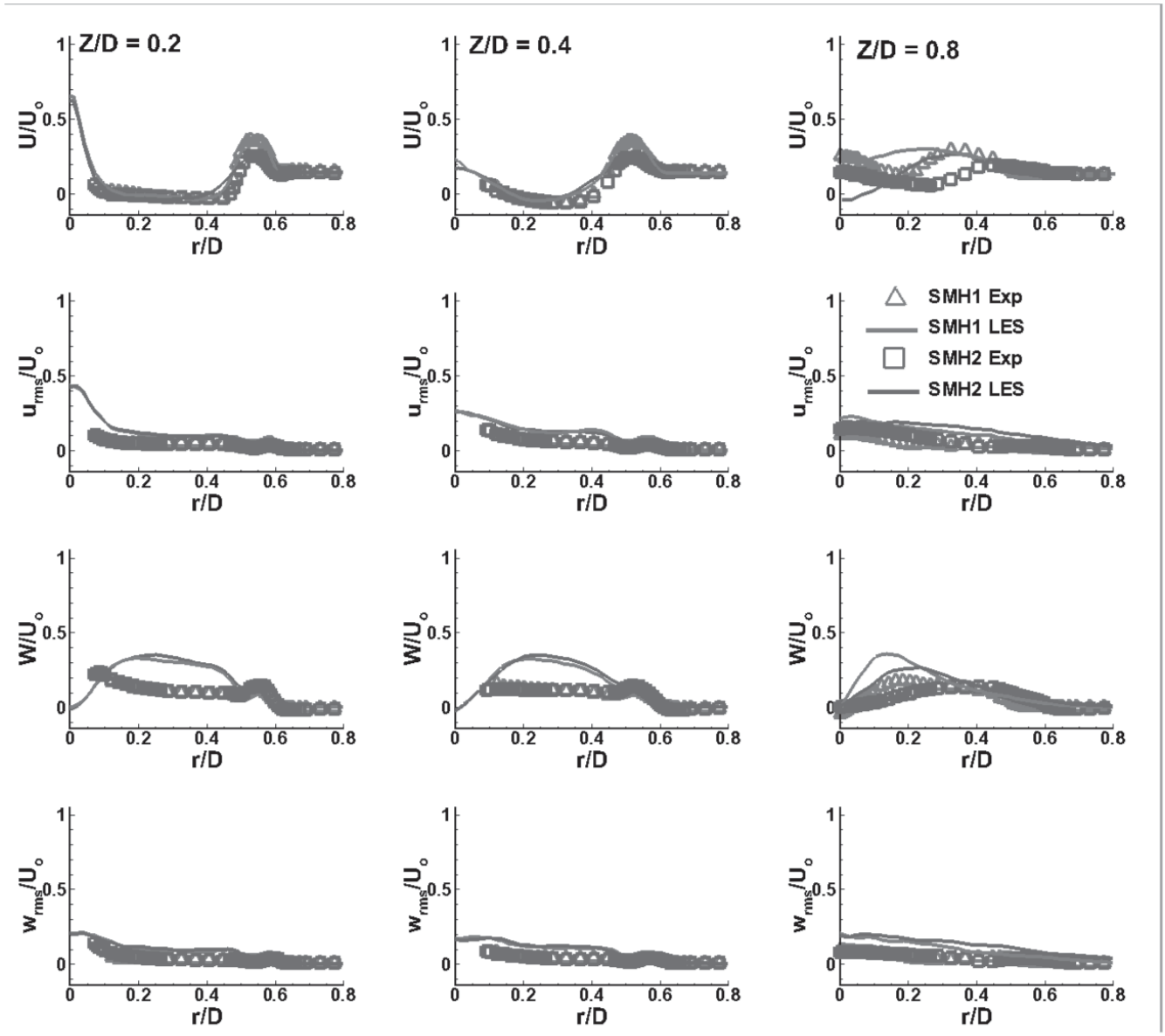

Figure 4(a): Radial Plot of Mean and rms velocity predictions for Hydrogen flames

Fig. 4(b) shows the temperature predictions in different downstream locations. In the upstream position, the temperature is over predicted till r/D=0.4. Then in the further radial positions, the predictions shows good match with the experimental measurements. The predictions improved along the downstream positions. There is an under prediction of mean mixture fraction in the central line. This creates the discrepancies in the temperature predictions. There are some discrepancies in the temperature and mean mixture fraction predictions but overall the predictions shows good agreement with the experimental measurements.

6.3.2 Analysis of Precessing Vortex core

Fig. 5 shows the PVC structure visualization of hydrogen flames. From the visualization of PVC structure, it is clear that even though the hydrogen flame is relatively longer than methane flame, qualitatively the vortex breakdown is much rapid in hydrogen flames. This can be attributed to high diffusivity of hydrogen fuel. In addition to that, the frequency of the oscillation is identified using FFT analysis. Interestingly, in spite of different boundary conditions, a peak frequency of around 48 Hz is

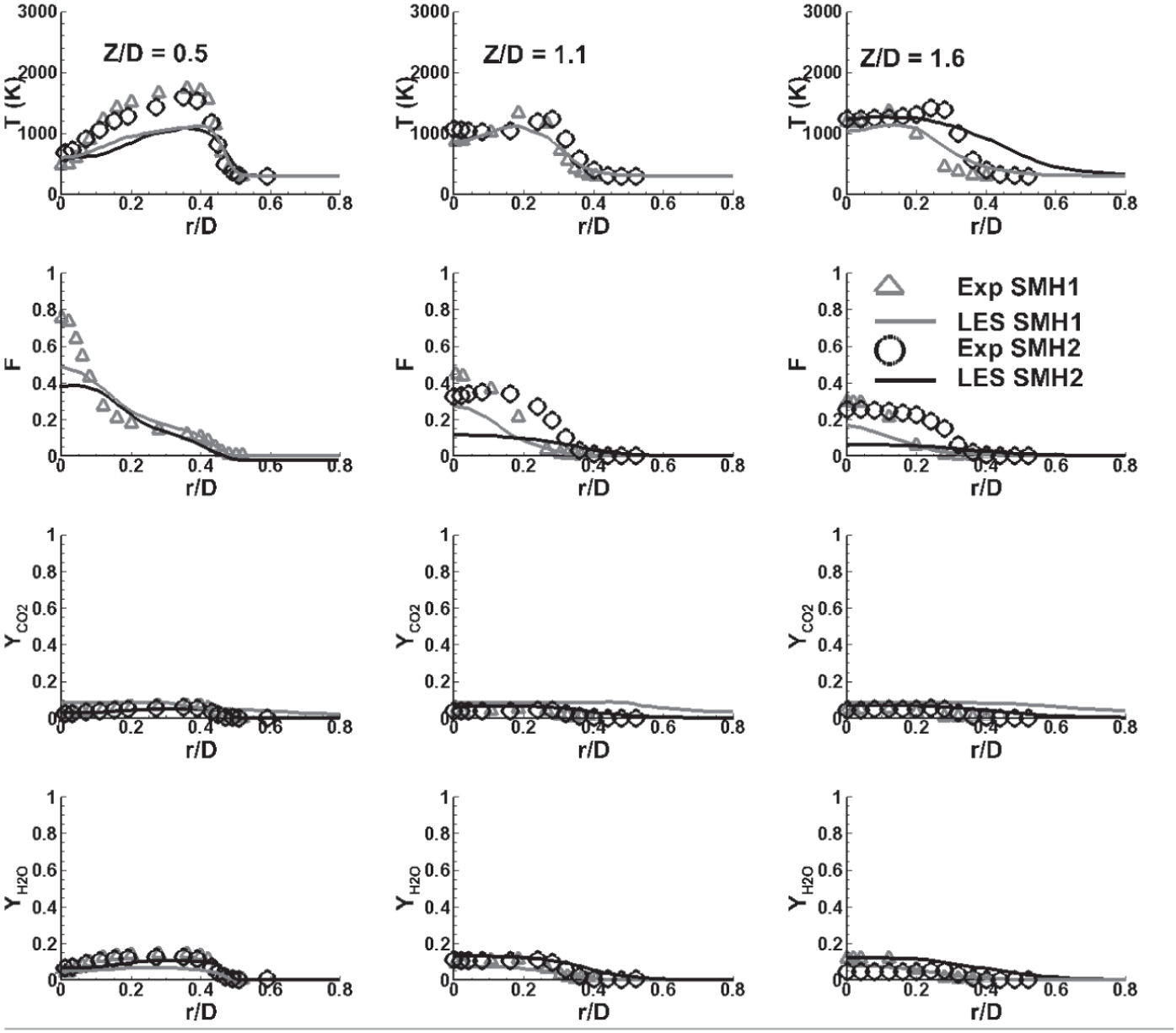

Figure 4(b): Radial Plot of Temperature (T), Mixure Fraction (F) and Mass Fraction predictions for Hydrogen flames

identified in all the three cases. However, there is a clear difference in the PVC structures of these three flames. Hence the phase averaged data is utilized to explore the PVC structures in details.

To reveal the inner structure of the PVC, five phases representing a complete cycle of the oscillating frequency is presented (Figs. 6(a-c)), and each phase is averaged over 4 complete cycles to remove high frequency oscillations. In SMH1 case, the vortices trailing from the swirling flow interacts with the bluff body induced vortices and then change its shape in phase 2. The interaction pattern is observed in the same manner for SMH2 case. Whereas in the SMH2 case, the vortices from the fuel jet is also interacts with swirling flow induced vortices. These vortices clearly change its shape through phase 3 and phase 4. Further, they regain their original shape as in phase 1, which finishes one complete cycle.

The SMH1 and SMH2 have same fuel jet velocity but different swirl velocity, whereas the SMH2 and SMH3 have same swirl velocity but different fuel jet velocity. The vortex breakdown is comparatively very high in SMH3 case. This shows the importance of fuel jet velocity in the characteristics of the flame. This can be seen in phase averaged data as well. In SMH3 case, where the fuel velocity is very high, through all the phases, the interaction between the vortices is concentrated only in the shear layer. Also, in both SMH1 and SMH3 case, the axial momentum flux is relatively higher compared with SMH2 case. So, as a consequence, in SMH2 case, the vortex trailing from the swirling jet, interacts with the vortex from fuel jet and grows in the size. This is reflected in the PVC structure visualization, where the vortex break down process is delayed in SMH2 case but it is very quick in both SMH1 and SMH3.

While comparing all three hydrogen cases, the repeating structures are mainly concentrated towards the outer shear layer, and the formation of PVC structure depends on the interaction of these structures with the incoming fuel jet. Though the shape and size of the inner vortical structures are different for three hydrogen flames, the interaction is mainly concentrated in the outer shear layer. The difference in the inner structures is responsible for the variation in PVC structures. However, as the mode of interaction is not similar in all the three flames, the oscillating frequency is same.

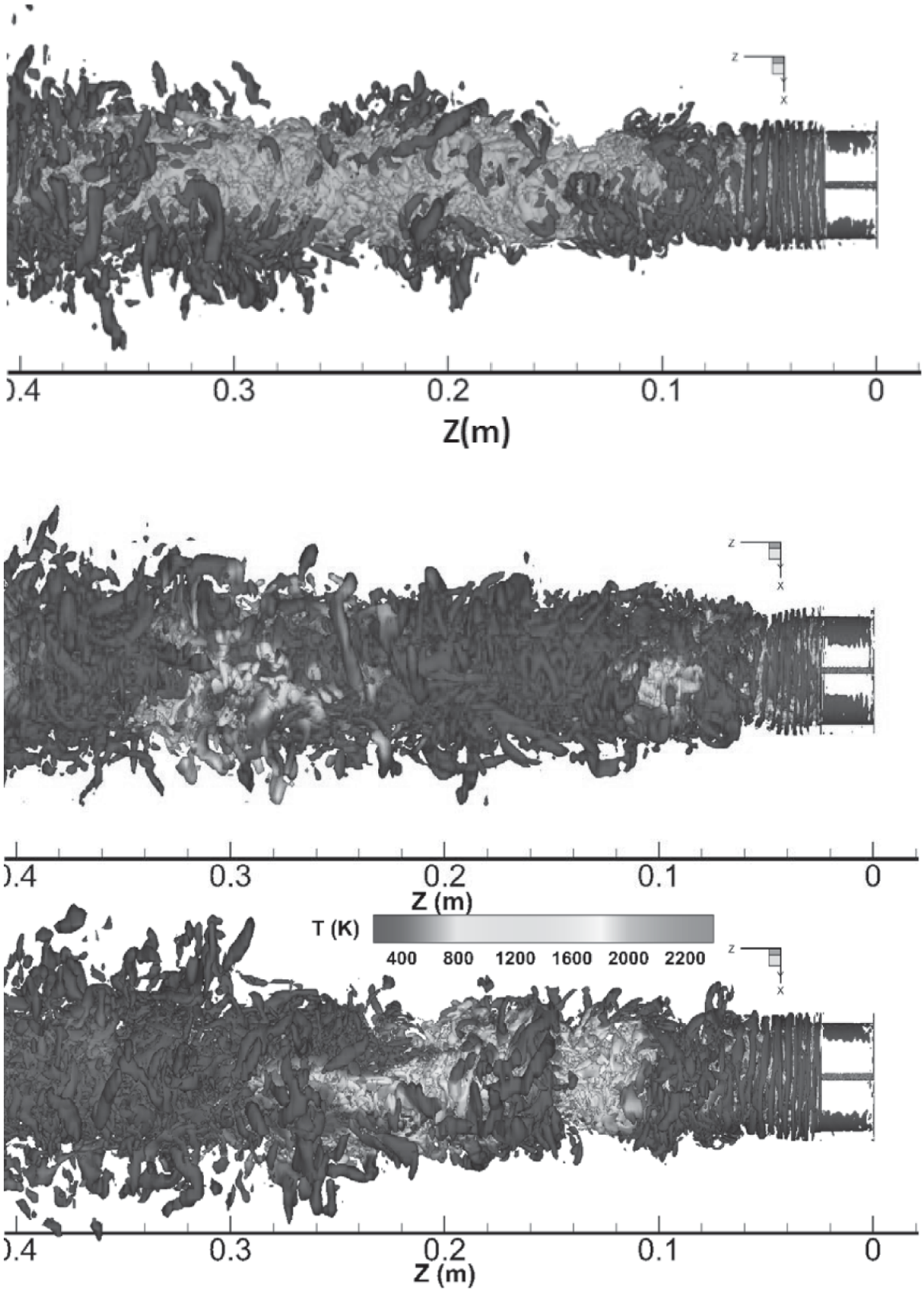

Figure 5: PVC visualization of SMH1, SMH2, SMH3 flames using Second Eigen Value method

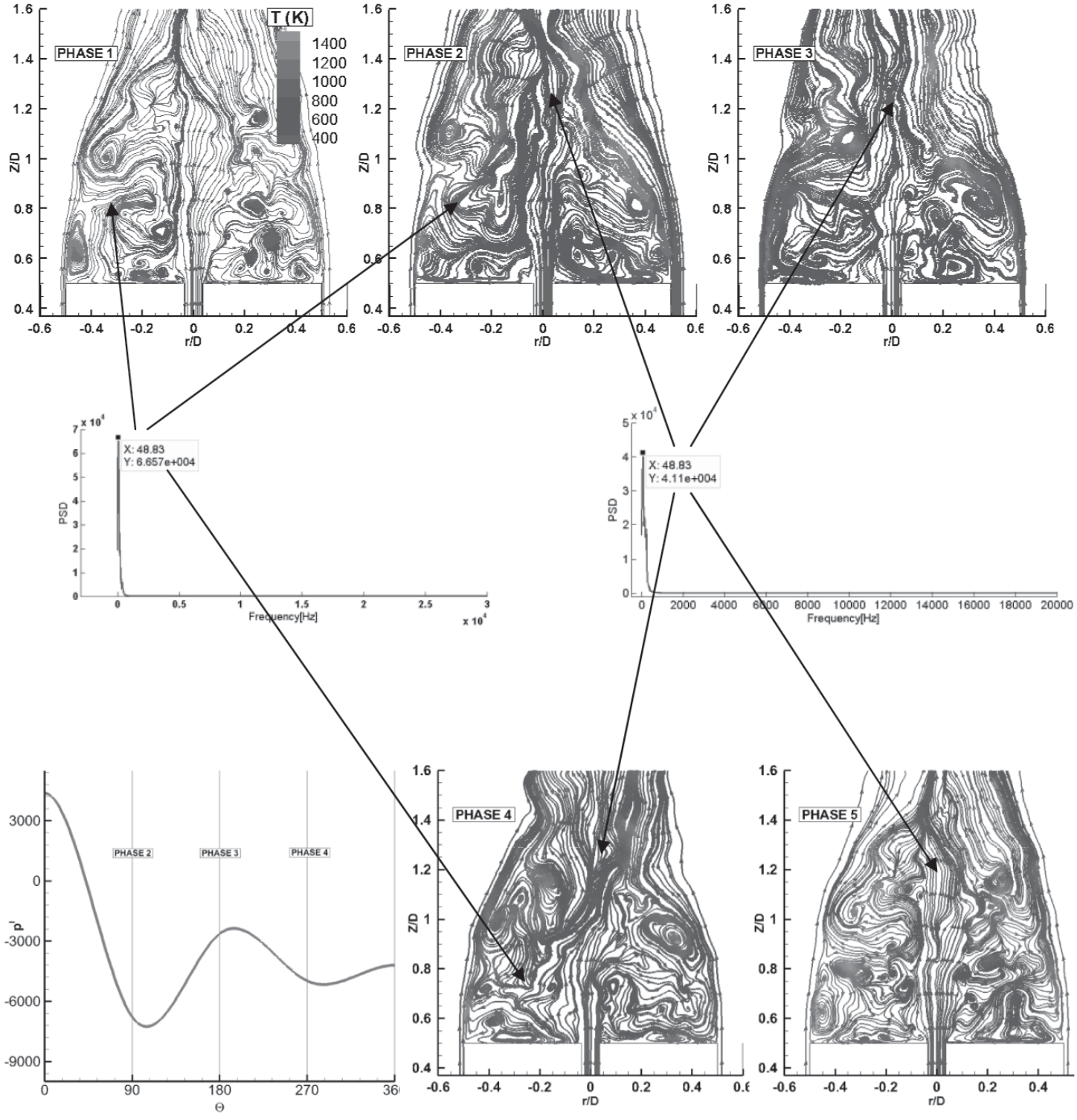

Figure 6(a): Phase averaged data for instantaneous flame from Phase 1-5 at an oscillation of 48 Hz for SMH1 flame

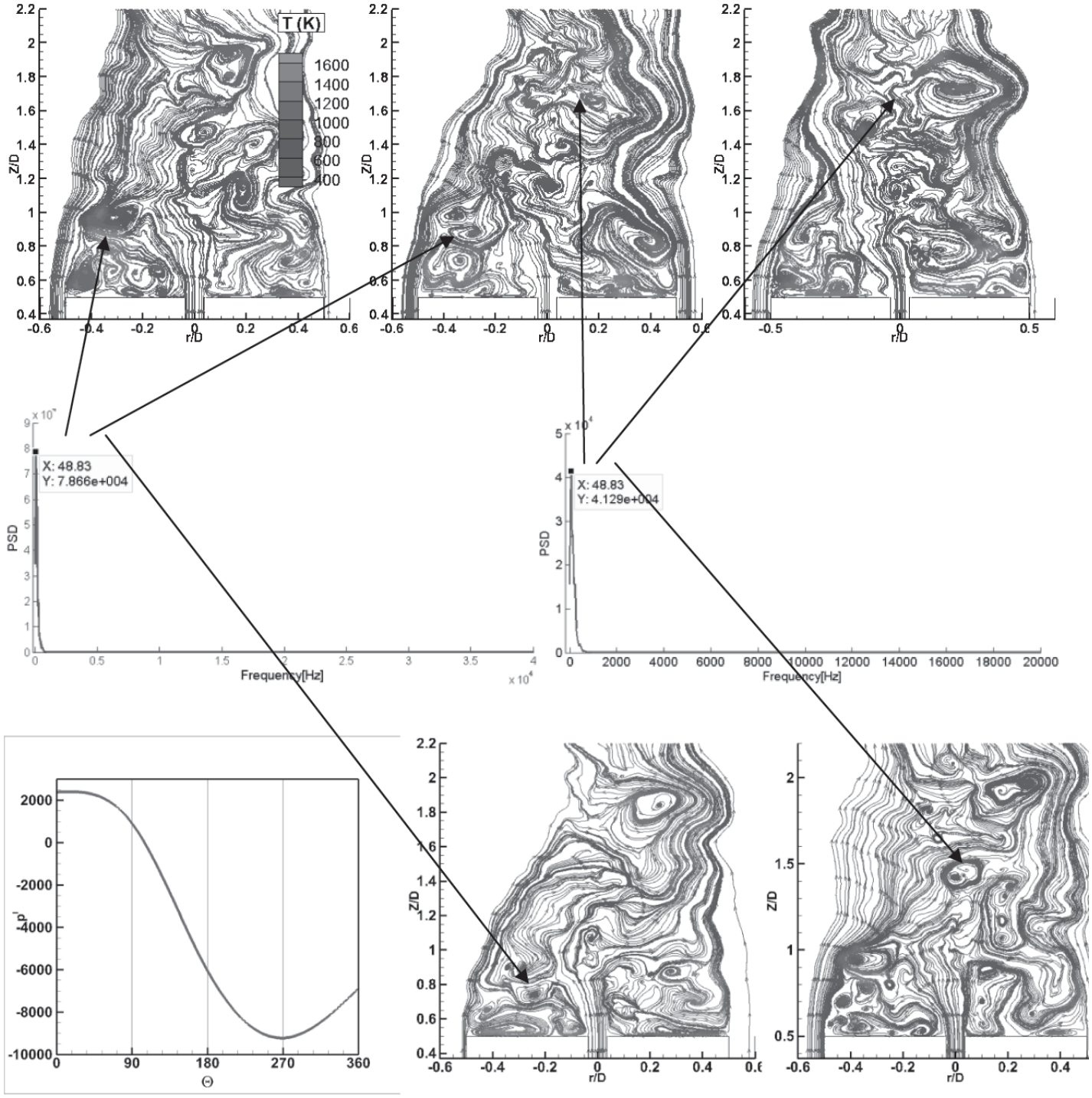

Figure 6(b): Phase averaged data for instantaneous flame from Phase 1-5 at an oscillation of 48 Hz for SMH2 flame

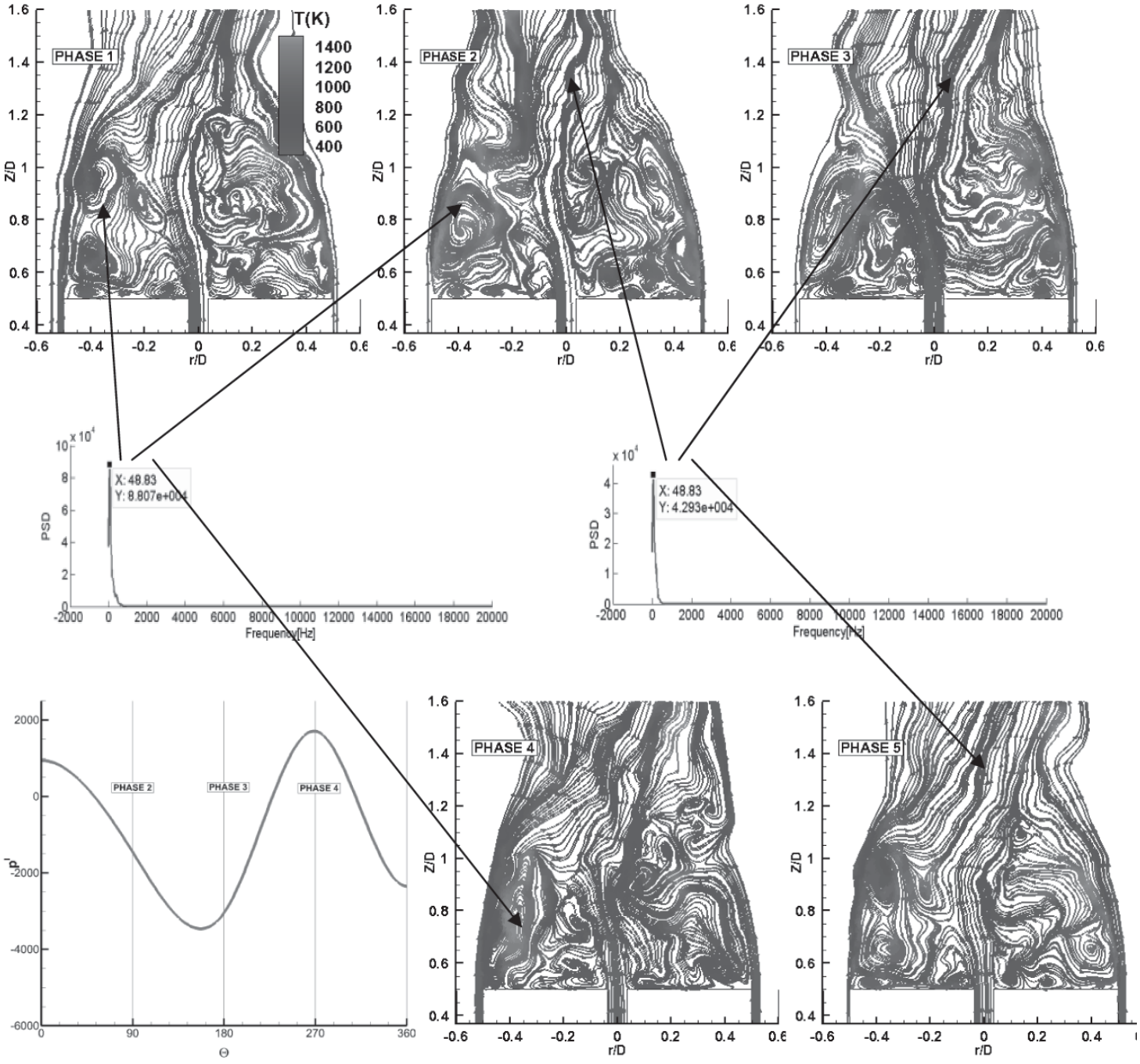

Figure 6(c): Phase averaged data for instantaneous flame from Phase 1-5 at an oscillation of 48 Hz for SMH3 flame

6 Conclusions

Large Eddy Simulation technique is successfully applied in studying the effect of swirl and fuel jet velocity in the instability characteristics of the hydrogen blended flames. The Precessing Vortex structure is explored using the second eigen value method. In the non reacting case, the vortex break down is very quick in the high swirl case, while the phase averaging technique explains the repeating structure responsible for the oscillation of PVC structure. In case of hydrogen flames, SMH1 and SMH3 cases shows quicker vortex breakdown process compared to SMH3 case. And the phase averaging technique reveals that the interaction between vortices is concentrated only in the shear layer in SMH1 and SMH3 case, where the axial momentum is high. And in SMH3 case, the shedding vortex from the swirl jet interacts with the vortex from the fuel jet and grows in size further and in turns causes the delay in vortex breakdown found in PVC structure. However, phase averaging technique further reveals that the mode of interaction between the coherent structures is identical for all the three hydrogen flames which causes the oscillating frequency to be same for all the three hydrogen flames.

Acknowledgment

The authors would like to acknowledge the IITK computer center (www.iitk.ac.in/cc) for providing the resources to perform the computation work, data analysis and article preparation.

References

1) Al-Abdeli, Y.M., Masri, A.R., 2003. Recirculation and Flow Field Regimes of Unconfined Non-Reacting Swirling Flows. Exp. Therm. Fluid Sci., 27(5), 655-665.
2) Al-Abdeli, Y.M., Masri, A.R., 2004. Precession and Recirculation in Turbulent Swirling Isothermal Jets'. Combust. Sci. Technol., 176(5-6), 645-665.
3) Al-Abdeli, Y.M., Masri, A.R., Marquez, G.R., Staner, S., 2006. Time-varying behaviour of turbulent swirling nonpremixed flames. Combust. Flame, 146(1), 200–214.
4) Ansys Fluent 15.0 User's Guide, 2010. Ansys Inc., Csnosburg, PA, USA.
5) Bhaya, R., De, A., Yadav, R., 2014. Large Eddy Simulation of Mild Combustion Using PDF-Based Turbulence-Chemistry Interaction Models. Combust. Sci. Technol., 186(9), 1138-1165.
6) Candel, S., Durox, D., Schuller, T., Bourgouin, J.F., Moeck, J.P., 2014. Dynamics of swirling flames. Annu. Rev. Fluid Mech., 46, 147-173.
7) Celik, I., Cehreli, Z., Yavuz, I., 2005. Index of resolution quality for large eddy simulation. J. Fluid Eng., 127, 949-58.
8) De, A., Acharya, S., 2012. Dynamics of upstream flame propagation in a hydrogen-enriched premixed flame. Int. J. Hydrog. Energ., 37(22), 17294-17309.
9)
10) De, A., Acharya, S., 2012. Parametric study of upstream flame propagation in hydrogen-enriched premixed combustion: Effects of swirl, geometry and premixedness. Int. J. Hydrog. Energ., 37(19), 14649-14668.
11) El-Asrag, H., Menon, S., 2005. Large Eddy Simulation of a Swirling Non-Premixed Flame. 41st AIAA/ASME/SAE/ASEE Jt. Propuls. Conf., Ariz., USA.
12) Germano, M., Piomelli, U., Moin, P., Cabot, W.H., 1991. A dynamic subgrid-scale eddy viscosity model. Phys. Fluids, A 3, 1760-1765.
13) Smith, G.P., Golden, D.M., Frenklach, M., Moriarty, N.W., Eiteneer, B., Goldenberg, M., Bowman, C.T., Hanson, R.K., Song, S., Gardiner Jr., W.C., Lissianski, V.V, Qin, Z., 1999. http://www.me.berkeley.edu/gri_mech/
14) Hu, L.Y., Zhou, L.X., Luo, Y.H., 2008. Large-eddy simulation of the Sydney swirling nonpremixed flame and validation of several subgrid-scale models. Numer. Heat Transf., Part B: Fundam., 53(1), 39-58.
15) James, S., Zhu, J., Anand, M.S., 2007. Large eddy simulations of turbulent flames using the filtered density function model. Proc. Combust. Inst., 31(2), 1737-1745.
16) Kempf, A., Malalasekera, W., Ranga Dinesh, K.K.J., Stein, O., 2008. Large eddy simulations of swirling non-premixed flames with flamelet models: a comparison of numerical methods. Flow Turbul. Combust., 81(4), 523-561.
17) Lilley, D.G., 1977. Swirl flows in combustion: A rev.. AIAA J, 15(8), 1063-78.
18) Malalasekera, W., Ranga Dinesh, K.K.J., Ibrahim, S.S., Masri, A.R., 2008. LES of Recirculation and Vortex Breakdown. Combust. Sci. Technol., 180(5), 809-32.
19) Malalasekera, W., Ibrahim, S.S., Masri, A.R., Sadasivuni, S.K., Gubba, S.R., 2010. Large eddy simulation of premixed and non-premixed combustion. Proc. of the 37th Natl. & 4th Int. Conf. on Fluid Mechanics and Fluid Power, Chennai, India.
20) Masri, A.R., Kalt, P.A.M., Barlow, R.S., 2004. The Compositional Structure of Swirl-Stabilised Turbulent Non-premixed Flames. Combust. Flame, 137(1), 1-37.
21) Pope, S.B., 2000. Turbulent Flows. Camb. Univ. Press, Camb., U. K.
22) Ranga Dinesh, K.K.J., Jiang, X., Kirkpatrick, M.P., Malalasekera, W., 2012. Combust. charact. of H2/N2 and H2/CO syngas nonpremixed flames. Int. J. Hydrog. Energ., 37(21), 16186-16200.
23) RangaDinesh, K.K.J., Malalasekera, W., Ibrahim, S.S., Kirkpatrick, M.P., 2006. Large eddy simulations of turbulent non-premixed swirling flames. Turbul., Heat and Mass Transf. (THMT05), Dubrovnik, HR.
24) RangaDinesh, K.K.J., Jenkins, K.W, Kirkpatrick, M.P., Malalasekera, W., 2009. Identification and analysis of instability in non-premixed swirling flames using LES. Combust. Theory Model, 13(6), 947-971.
25) RangaDinesh, K.K.J., Kirkpatrick, M.P., 2009. Study of jet precession, recirculation and vortex breakdown in turbulent swirling jets using LES. Comput. Fluids, 38(6), 1232-1242.
26) RangaDinesh, K.K.J., Malalasekera, W., Ibrahim, S.S., Kirkpatrick, M.P., 2005. Large Eddy Simulation of isothermal flows. 5th Asia-Pac. conf. on combust., Univ. of Adel., Adel., Aust..
27) Stien, O., Kempf, A., 2007. LES of the Sydney swirl flame series: A study of vortex breakdown in isothermal and reacting flows. Proc. Combust. Inst., 31, 1755-1763.
28) Smagorinsky, J., 1963. General circulation experiments with the primitive equations. I. The basic experiment. Mon. Weather Rev., 91(3), 99-164.
29) Syred, N., Beer, J.M., 1974. Combustion in swirling flows: a review. Combust. and Flame, 23(2), 143-201.
30) Yang, Y., Søren, K.K., 2012. Comparison of Reynolds Averaged Navier-Stokes Based Simulation and Large-eddy Simulation for One Isothermal Swirling Flow. J. Therm. Sci., 21(2), 154-61.
31) Yang, Y., Søren, K.K., 2012. Large-eddy simulations of the non-reactive flow in the Sydney Swirl burner. Int. J. Heat Fluid Flow, 36, 47-57.